Computation of spectroscopic factors with the coupled-cluster method

Ø. Jensen,[1,*] G. Hagen,[2] T. Papenbrock,[2,3] D. J. Dean,[2] and J. S. Vaagen[1]
[1]*Department of Physics and Technology, University of Bergen, N-5007 Bergen, Norway*
[2]*Physics Division, Oak Ridge National Laboratory, Oak Ridge, Tennessee 37831, USA*
[3]*Department of Physics and Astronomy, University of Tennessee, Knoxville, Tennessee 37996, USA*
(Received 16 April 2010; published 19 July 2010)

We present a calculation of spectroscopic factors within coupled-cluster theory. Our derivation of algebraic equations for the one-body overlap functions are based on coupled-cluster equation-of-motion solutions for the ground and excited states of the doubly magic nucleus with mass number A and the odd-mass neighbor with mass $A-1$. As a proof-of-principle calculation, we consider ^{16}O as well as the odd neighbors ^{15}O and ^{15}N and compute the spectroscopic factor for nucleon removal from ^{16}O. We employ a renormalized low-momentum interaction of the $V_{\text{low-}k}$ type derived from a chiral interaction at next-to-next-to-next-to-leading order. We study the sensitivity of our results by variation of the momentum cutoff and then discuss the treatment of the center of mass.

DOI: 10.1103/PhysRevC.82.014310 PACS number(s): 21.10.Jx, 21.60.De, 21.60.Gx, 31.15.bw

I. INTRODUCTION

In the past two decades, *ab initio* nuclear structure calculations have led to the development and test of high-precision models with predictive power [1–3]. Recently, the application of effective field theory (EFT) [4–7] and renormalization-group techniques [8,9] has resulted in a model-independent approach to the nuclear interaction. These approaches have significantly deepened our understanding of nuclear forces and have also provided us with new technical means to simplify the solution of the nuclear many-body problem. The interactions from chiral EFT have been probed in light nuclei [10–13] and selected medium-mass nuclei using different techniques [14–16]. The focus of *ab initio* calculations is not only on observables such as binding energies, radii, and low-lying excitation spectra, but also on transition rates and more detailed spectroscopic information. Very recently, *ab initio* theory began to bridge the gap from nuclear structure to reactions [17–19]. The inclusion of continuum effects, for instance, is necessary for the description of weakly bound and unbound nuclei. Direct reactions such as stripping and pickup of a single nucleon are rather well understood within phenomenological approaches (see, e.g., Ref. [20]) but constitute a current frontier for *ab initio* theory.

The interpretation of direct reactions within a given model or Hamiltonian is based on spectroscopic factors [21,22]. The spectroscopic factor depends on wave function overlaps [see Eq. (16) for a definition] and provides useful information that relates nuclear structure within a given model (i.e., within a given Hamiltonian) to stripping and transfer reactions [21]. The spectroscopic factor is not an observable, as it depends on the employed Hamiltonian or model. In nuclear physics, the high-momentum parts of the interaction are unconstrained and modeled in different ways. Thus, the short-ranged part of the wave function is model dependent, and so is an overlap between wave functions. Therefore, the spectroscopic factor is merely a theoretical quantity and cannot be measured [23,24]. However, the spectroscopic factor "provides a useful basis for the comparison of experiment and current nuclear models" [21]. Its purpose thus lies in understanding a direct reaction within a certain model or Hamiltonian, and this interpretation might be useful and interesting [25–29].

In this paper, we develop the technical tools to compute spectroscopic factors within the coupled-cluster method [30–34] (see Ref. [35] for a recent review of this method) and perform a proof-of-principle calculation for ^{16}O. The computation of the spectroscopic factor within coupled-cluster theory is not trivial (i) because the method does not readily yield a many-body wave function and (ii) owing to details related to the translation invariance of the coupled-cluster wave function. However, the coupled-cluster method can employ modern nonlocal potentials [6–9], reaches medium-mass nuclei [14], and has been extended to treat weakly bound and unbound nuclei [17] that are of current experimental interest. This paper is structured as follows. Section II is dedicated to a summary of the employed coupled-cluster method. The theoretical computation of spectroscopic factors within coupled-cluster theory is presented in Sec. III. We present our results and a discussion of the center-of-mass treatment in Sec. IV. Section V reports our conclusions and an outlook.

II. EQUATION-OF-MOTION AND COUPLED-CLUSTER THEORY FOR NUCLEI

In this section we introduce the Hamiltonian and coupled-cluster theory [30–34] for closed-shell and open-shell nuclei. Although our implementation of coupled-cluster theory has been presented elsewhere [14,35–38], we give a brief overview of the method, as some details are needed for the calculation of spectroscopic factors.

We consider the intrinsic nuclear A-body Hamiltonian,

$$\hat{H} = \hat{T} - \hat{T}_{\text{c.m.}} + \hat{V} = \sum_{1\leqslant i<j\leqslant A} \frac{(\vec{p}_i - \vec{p}_j)^2}{2mA} + \hat{V}. \qquad (1)$$

*oyvind.jensen@uib.no

Here T is the kinetic energy, $T_{\text{c.m.}}$ is the kinetic energy of the center-of-mass coordinate, and V is the two-body nucleon-nucleon interaction. In this paper we use low-momentum interactions $V_{\text{low-}k}$ [9,39] with sharp cutoffs $\lambda = 1.6$, 1.8, 2.0, and 2.2 fm^{-1}, respectively. For simplicity, we neglect any contributions of three-nucleon forces, as we focus on a proof-of-principle calculation.

In coupled-cluster theory, one writes the ground-state many-body wave function as

$$|\psi_0\rangle = e^T |\phi_0\rangle. \tag{2}$$

Here, $|\phi_0\rangle$ is a product state. The cluster operator T introduces correlations as a linear combination of particle-hole excitations,

$$T = T_1 + T_2 + \cdots + T_A. \tag{3}$$

Here, the n-particle–n-hole excitation operator is

$$T_n = \left(\frac{1}{n!}\right)^2 \prod_{\nu=1}^{n} \sum_{a_\nu, i_\nu} t_{i_1 \cdots i_n}^{a_1 \cdots a_n} a_{a_1}^\dagger \cdots a_{a_n}^\dagger a_{i_n} \cdots a_{i_1}. \tag{4}$$

We employ the standard convention that indices $ijk\ldots$ refer to orbits below Fermi level (holes), and indices $abc\ldots$ to orbits above Fermi level (particles). Approximations in coupled-cluster theory are introduced by truncating the cluster operator T at a certain particle-hole excitation level. In this work we truncate T at the two-particle–two-hole excitation level, that is, $T \approx T_1 + T_2$, which gives the coupled-cluster method with singles and doubles excitations (CCSD). This is the most commonly used approximation, as it provides a good compromise between computational cost, on the one hand, and accuracy, on the other.

Within the CCSD approximation, the computational cost is given by $n_o^2 n_u^4$, where n_o and n_u denote the number of occupied and unoccupied orbitals, respectively. The correlated ground-state solution is given by the amplitudes t_i^a and t_{ij}^{ab} that solve the nonlinear equations

$$\langle \phi_i^a | \overline{H} | \phi_0 \rangle = 0, \tag{5}$$

$$\langle \phi_{ij}^{ab} | \overline{H} | \phi_0 \rangle = 0. \tag{6}$$

Here, the bra states are particle-hole excitations of the reference Slater determinant, and $\overline{H}$ denotes the similarity-transformed Hamiltonian,

$$\overline{H} = e^{-T} H e^T = (H e^T)_c. \tag{7}$$

The subscript c indicates that only fully connected diagrams give nonzero contributions. Once T is determined from the solution of the coupled-cluster equations (5) and (6), the correlated ground-state energy is given by

$$E_0 = \langle \phi_0 | \overline{H} | \phi_0 \rangle. \tag{8}$$

The CCSD approach is known to work particularly well for the ground state of nuclei with closed (sub-)shells, as a Slater determinant provides a reasonable first approximation. In this work we use the equation-of-motion (EOM) [35,40–43] method to solve for the ground and excited states of the closed-shell nucleus A and its odd neighbors with mass number $A-1$.

In the EOM, the ground and excited states of a nucleus with mass number B are obtained by acting with an excitation operator Ω_μ on the ground-state wave function of a nucleus with mass number A, that is, $\psi_\mu^B = \Omega_\mu \psi_0^A$. Here μ denotes quantum numbers such as spin, parity, and isospin projection. Within the EOM approach, the ground-state wave function ψ_0^A denotes the coupled-cluster wave function $e^T \phi_0$. In this work we choose either $B = A$, in which case we solve the excited states of the closed-shell nucleus A, or $B = A-1$, in which case we solve the ground and excited states of the $A-1$ neighboring nucleus. We refer to EOM with a particle removal operator as PR-EOM. To solve for the excited states of the closed-shell nucleus A, we define Ω_μ by the excitation operators,

$$R^A = r_0 + \sum_{ia} r_i^a a_a^\dagger a_i + \frac{1}{4} \sum_{ijab} r_{ij}^{ab} a_a^\dagger a_b^\dagger a_j a_i, \tag{9}$$

$$L^A = 1 + \sum_{ia} l_a^i a_i^\dagger a_a + \frac{1}{4} \sum_{ijab} l_{ab}^{ij} a_i^\dagger a_j^\dagger a_b a_a. \tag{10}$$

Here, we suppressed the index μ, but it is understood that the operators R^A and L^A excite and de-excite states with quantum numbers μ, respectively. For the ground and excited states of the nucleus with mass number $A-1$, we define Ω_μ by the particle removal operators,

$$R^{A-1} = \sum_i r_i a_i + \frac{1}{2} \sum_{ija} r_{ij}^a a_a^\dagger a_j a_i, \tag{11}$$

$$L^{A-1} = \sum_i l^i a_i^\dagger + \frac{1}{2} \sum_{ija} l_a^{ij} a_i^\dagger a_j^\dagger a_a. \tag{12}$$

Again, we supressed the index μ labeling the quantum numbers. The operators $R_\mu = R^A$ ($R_\mu = R^{A-1}$) commute with the cluster operator T, and the unknowns r_i^a, r_{ij}^{ab} (r_i, r_{ij}^a) solve the EOM,

$$[\overline{H}, R_\mu] |\phi_0\rangle = \omega_\mu R_\mu |\phi_0\rangle, \tag{13}$$

which defines an eigenvalue problem for the excitation operator R_μ with eigenvalue $\omega_\mu = E_\mu - E_0$. It is clear from definitions (4) and (7) that $\overline{H}$ is non-Hermitian; dual-space solutions need to be calculated explicitly. We obtain the de-excitation operators $L_\mu = L^A, L^{A-1}$ by solving the left eigenvalue problem,

$$\langle \phi_0 | L_\mu \overline{H} = \langle \phi_0 | L_\mu \omega_\mu. \tag{14}$$

The right and left eigenvectors form a biorthogonal set and are normalized in the following way:

$$\langle \phi_0 | L_\mu R_{\mu'} | \phi_0 \rangle = \delta_{\mu\mu'}. \tag{15}$$

The EOM solution for the ground state of system A is identical to the CC solution, so that $R_0^A = r_0 = 1$. Reference [35] provides a detailed description of the EOM.

III. OVERLAP FUNCTIONS AND SPECTROSCOPIC FACTORS FROM COUPLED-CLUSTER THEORY

The one-particle overlap function between two wave functions Ψ_{A-1} and Ψ_A of nuclei with mass number $A-1$

and A, respectively, is defined as [22]

$$O^A_{A-1}(\vec{x}) \equiv \sqrt{A}\int \mathrm{d}^{3(A-2)}\xi\, \Psi^*_{A-1}(\vec{\xi})\Psi_A(\vec{x},\vec{\xi}). \quad (16)$$

Here ξ represent the $3(A-2)$ translationally invariant position coordinates and the $A-1$ spin coordinates of $A-1$ particles present in both Ψ_{A-1} and Ψ_A, while $\vec{x}$ labels the position and spin of the additional particle in the nucleus with mass number A with respect to the center of mass of the nucleus with mass number $A-1$. The isospin coordinate has been suppressed.

In our coupled-cluster approach, however, we do not employ coordinates with respect to the center of mass, as this would limit us to light systems [44]. For this reason, the overlap is associated with a specific nucleon represented by a second quantization operator,

$$O^A_{A-1}(\vec{x}) \equiv \langle A-1|a(\vec{x})|A\rangle. \quad (17)$$

Here, $|A\rangle$ and $|A-1\rangle$ denote eigenstates in the nucleus with mass A and $A-1$, respectively. A few comments regarding the center of mass are in order. First, Eq. (16) describes the removal of a particle with respect to the center of mass, while Eq. (17) simply removes a particle at position $\vec{x}$. In principle, the removal of a particle with respect to the center of mass can be expanded in terms of single-particle annihilation and creation operators with the leading term being of the form of Eq. (17) [45]. Such an expansion is in powers of $1/A$ and we thus consider its leading term. Second, the states $|A\rangle$, $|A-1\rangle$ need to factorize into a product of an intrinsic wave function and a center-of-mass wave function. In Sec. IV we show that this is indeed the case. This factorization is caused by the usage of the intrinsic Hamiltonian (1) and the employment of a sufficiently large model space [46]. In small spaces, one needs to explicitly remove spurious center-of-mass effects [28,47].

In Eq. (17) $|A\rangle$ typically denotes the ground state, while $|A-1\rangle$ is the ground state or an excited state. Our formalism will be kept general and is not limited to these cases. The radial overlap function $O^A_{A-1}(lj;r)$ is derived by expanding $\vec{x}$ in terms of partial waves,

$$a(\vec{x}) = (-)^{j-m}\sum_{ljm}\tilde{a}_{lj-m}(r)Y_{ljm}(\hat{x}). \quad (18)$$

Here, $Y_{ljm}(\hat{x})$ is the spin-orbital spherical harmonic,

$$Y_{ljm}(\hat{x}) = [Y_l(\hat{r})\otimes\chi_{1/2}(\sigma)]_{jm},$$

$Y_l(\hat{r})$ is the spherical harmonic of rank l and $\chi_{1/2}(\sigma)$ is a fermionic spin function. The orbital angular momentum quantum number is denoted l, while j and m denote the rank and projection, respectively, of $Y_{ljm}(\hat{x})$ as a spherical tensor. The hat denotes unit vectors, that is, $\hat{x}\equiv\vec{x}/|\vec{x}|$. We have also introduced the spherical annihilation operator $\tilde{a}_{ljm}(r) = (-)^{j+m}a_{lj-m}(r)$. The radial overlap is now given by the reduced matrix element and the overlap becomes[1]

$$O^A_{A-1}(\vec{x}) = \sum_j (-)^{j-m}(J_AM_Aj-m \mid J_{A-1}M_{A-1}) \times O^A_{A-1}(lj;r)Y_{ljm}(\hat{x}). \quad (19)$$

[1]Many authors use an alternative definition derived from $\langle A|a^\dagger(\vec{x})|A-1\rangle$.

Here, $(\cdot\mid\cdot)$ denotes a Clebsch-Gordan coefficient. The overlap is now expressed by a radial function associated with each tensorial component $Y_{ljm}(\hat{x})$,

$$O^A_{A-1}(lj;r) \equiv \langle A-1||\tilde{a}_{lj}(r)||A\rangle = (-)^{j-m}\frac{\langle A-1M_{A-1}|a_{ljm}(r)|AM_A\rangle}{(J_AM_Aj-m \mid J_{A-1}M_{A-1})}. \quad (20)$$

This equation also defines the reduced matrix elements we employ.

The norm of the radial overlap function is the spectroscopic factor

$$S^A_{A-1}(lj) = \int \mathrm{d}r r^2\left|O^A_{A-1}(lj;r)\right|^2. \quad (21)$$

The overlap functions can be expressed in an energy basis by inserting the expansions

$$a^\dagger_{ljm}(r) = \sum_n a^\dagger_{nljm}\phi_{nlj}(r), \quad (22)$$

$$a_{ljm}(r) = \sum_n a_{nljm}\phi^*_{nlj}(r), \quad (23)$$

where n is the nodal quantum number and $\phi_{nlj}(r)$ is the radial single-particle wave function associated with the orbits $nljm$. While $a^\dagger_{ljm}(r)$ represents the creation of a particle at radial distance r, $a^\dagger_{nljm}$ represents the action of populating a single-particle orbit.

Assuming orthogonality of the single-particle wave functions, the spectroscopic factor is written as

$$S^A_{A-1}(lj) = \sum_n |\langle A-1||\tilde{a}_{nlj}||A\rangle|^2 = \sum_n \frac{|\langle A-1|a_{nljm}|A\rangle|^2}{(J_AM_Aj-m \mid J_{A-1}M_{A-1})^2}. \quad (24)$$

Here we used the Wigner-Eckhart theorem for the reduced matrix elements. Equation (24) is our starting point, as we work in an uncoupled (m-scheme) basis. Using the EOM-CCSD solutions for the right and left eigenvalue problems for the A and the $A-1$ systems, and employing the ground-state solutions for system A, Eq. (24) takes the form

$$S^A_{A-1}(lj) = \sum_n \frac{\langle\phi_0|L^A_0\overline{a^\dagger_{nljm}}R^{A-1}_\mu|\phi_0\rangle\,\langle\phi_0|L^{A-1}_\mu\overline{a_{nljm}}R^A_0|\phi_0\rangle}{(J_AM_Aj-m \mid J_{A-1}M_{A-1})^2}. \quad (25)$$

This gives the equation for the spectroscopic factors as defined within coupled-cluster theory. We note that this equation is unambiguously and uniquely defined in terms of the left and right eigenstates of the nuclei with mass numbers A and $A-1$. This is clear, as the spectroscopic factor is given by the absolute value squared of the one-body overlap matrix element, so any ambiguity related to the normalization condition (15) is removed.

In Eq. (25) we have introduced the similarity-transformed creation and annihilation operators,

$$\overline{a^\dagger_p} = e^{-T}a^\dagger_p e^T, \quad (26)$$

$$\overline{a_p} = e^{-T}a_p e^T. \quad (27)$$

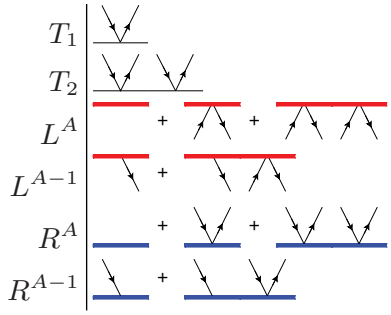

FIG. 1. (Color online) Left: Algebraic symbols for the particle-hole excitation operators and particle removal operators. Right: Corresponding diagrammatic representations. Arrows pointing up (down) represent particle (hole) orbits with implicit summation indices $a, b, c, \ldots$ $(i, j, k, \ldots)$.

Using the Baker-Campbell-Hausdorff commutator expansion, we can derive algebraic expressions for $\overline{a_p^\dagger}$ and $\overline{a_p}$ in terms of the "bare" creation and annihilation operators $a_p^\dagger$ and a_p and the particle-hole excitations amplitudes t_i^a and t_{ij}^{ab},

$$\overline{a_p^\dagger} = a_p^\dagger - \sum_b t_p^b a_b^\dagger - \frac{1}{2}\sum_{jbc} t_{pj}^{bc} a_b^\dagger a_c^\dagger a_j, \tag{28}$$

$$\overline{a_p} = a_p + \sum_i t_i^p a_i + \frac{1}{2}\sum_{ijc} t_{ij}^{pc} a_c^\dagger a_j a_i. \tag{29}$$

These equations can also be given in diagrammatic form, which provides a convenient bookkeeping system for the available Wick contractions in the expressions.

The coupled-cluster diagrams are similar to Goldstone diagrams. An algebraic Wick contraction corresponds to the diagrammatic connection of two directed lines, but the interpretation rules are slightly different. We refer the reader to Refs. [35] and [48] for a complete introduction to the diagrammatic approach. Here we only present the few concepts necessary to introduce the novel extensions of the formalism used in the context of spectroscopic factors.

Diagrammatic representations of the excitation and particle-removal operators T, L_μ, and R_μ are displayed in Fig. 1. Lines with arrows pointing up (down) represent particle (hole) orbits. These lines have implicit indices $a, b, c, \ldots$ $(i.j, k, \ldots)$ that are summed over. We suppress both the summation symbol and the dummy indices for a cleaner notation.

We have to deal with diagrams that represent operators with an index that is not being summed over. Such a creation (annihilation) operator is represented by a directed line pointing out from (into) a small circular vertex. The corresponding diagrams are displayed in the upper half of Fig. 2. Equations (28) and (29) can be reproduced diagrammatically as displayed in the lower half of Fig. 2. The possible Wick contractions between the creation and annihilation operators $a_p^\dagger$ and a_p and the cluster operators T_1 and T_2 depend on whether the index p denotes an orbital above or below the Fermi surface. The small circular vertices distinguish the index fixed by the operator and is not summed over. In practice, the circle prevents an accidental connection of the operator line,

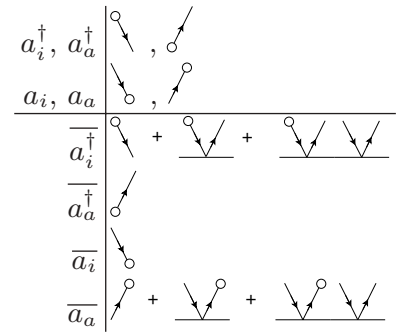

FIG. 2. Diagrammatic representation of the "bare" and the similarity-transformed second quantization operators. The horizontal bars represent the cluster operators T_1 and T_2, as displayed in Fig. 1.

which would have introduced an erroneous Wick contraction when the spectroscopic factor diagrams are written down.

The overall sign of a diagram is determined according to standard rules [48]. The negative sign of the second and third terms in Eq. (28) is reflected in the $\overline{a_i^\dagger}$ diagrams by the internal hole lines that connect the small open circle with the T operators. To determine the overall sign correctly for the spectroscopic factor diagrams, a sequence of directed lines ending or starting in a small circular vertex must be counted as a loop.

The diagrams in Figs. 1 and 2 are the basic building blocks for computation of the spectroscopic factor. We compute the matrix elements of the overlap function as products of the components R_μ, L_μ, and either $\overline{a_p^\dagger}$ or $\overline{a_p}$. The only nonvanishing contributions to the spectroscopic factor come from the diagrams in which all directed lines can be connected. These diagrams and the corresponding algebraic interpretation are shown in Fig. 3. We assume an implicit summation over repeated indices.

The computational cost of the spectroscopic factor diagrams has the very gentle scaling $n_o^2 n_u^2$, so the cost is completely dominated by the coupled-cluster and EOM calculations. In the case that $|A\rangle$ is the ground state of the closed-shell nucleus, we have $r_i^a = 0 = r_{ij}^{ab}$, and several diagrams vanish.

IV. RESULTS

In this section we present our results for the calculation of the spectroscopic factor using *ab initio* coupled-cluster theory. We study the spectroscopic factor of nucleon removal from ^{16}O by calculating the one-body overlap functions of ^{16}O with the odd-mass neighbors ^{15}O and ^{15}N using the (PR-)EOM-CCSD approach to the ground and excited states of the $A-1$ nuclei. The CCSD approximation is used to calculate the ground state of ^{16}O.

Our model space is spanned by oscillator states. We label the model space with the largest principal quantum number N that is included in the single-particle basis, so that the maximum single-particle energy is $E_N = (N + \frac{3}{2})\hbar\omega$, and the number of major oscillator shells is $N + 1$. In Fig. 4 we show the convergence of the ground state of ^{16}O with increasing size of the model space for a wide range of oscillator frequencies $\hbar\omega$, using $V_{\text{low-}k}$ with momentum cutoff $\lambda = 2.0$ fm^{-1}. In Fig. 5

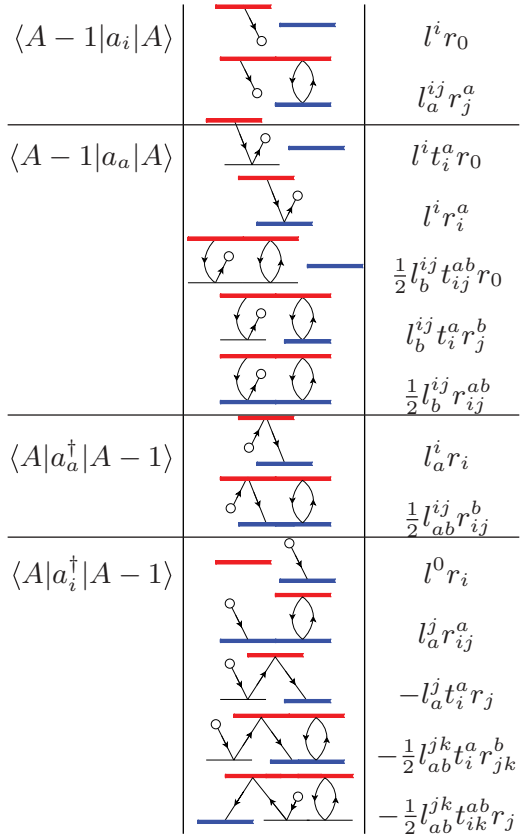

FIG. 3. (Color online) Diagrammatic representation of the overlap expressions; repeated indices imply a summation. If the closed-shell system is in the ground state, diagrams involving either r_i^a or r_{ij}^{ab} vanish. The individual components of these diagrams are explained in the captions to Figs. 1 and 2.

we show the convergence of the ground-state energies of ^{15}O and ^{15}N relative to the ground-state energy of ^{16}O.

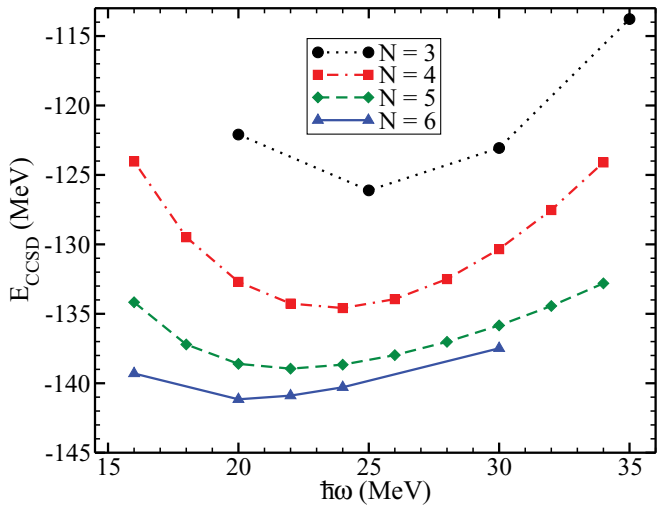

FIG. 4. (Color online) Convergence of the ground-state energy (within the CCSD) of ^{16}O using a low-momentum potential with cutoff $\lambda = 2.0$ fm^{-1} for increasing model space size $N = 2n + l$ and as a function of the oscillator spacing $\hbar\omega$.

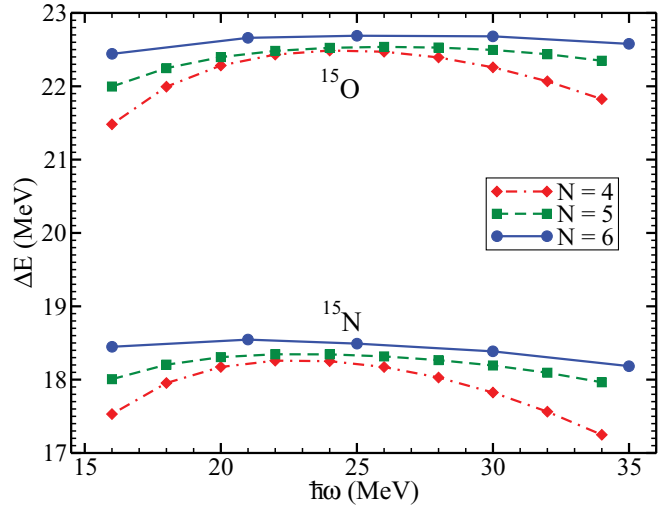

FIG. 5. (Color online) Convergence of the ground-state energies (within the PR-EOM-CCSD) of ^{15}O and ^{15}N relative to the ground-state energy of ^{16}O using a low-momentum potential with cutoff $\lambda = 2.0$ fm^{-1} for increasing model space size and as a function of the oscillator spacing $\hbar\omega$.

Our results shown in Figs. 4 and 5 show a weak dependence on $\hbar\omega$ in the largest model space. We estimate that our results for the ground-state energies are converged within a few mega–electron volts in our largest model. We note that the CCSD ground state for ^{16}O is overbound by ∼15 MeV compared to experiment and that the $A = 15$ nuclei lack about 6 MeV of binding energy with respect to ^{16}O. However, the energy difference between the ground state of ^{15}O and that of ^{15}N is ∼4 MeV, which is very close to the experimental value of 3.5 MeV. The main deficiency of our calculation is the omission of three-nucleon forces. The leading-order contributions of these forces are isospin symmetric [49], and it seems that this is the reason for the relatively good reproduction of the energy difference between the two $A = 15$ nuclei.

The $\hbar\omega$ dependence provides some information about how the finite size of the model space affects the solutions. For high values of $\hbar\omega$, the model space includes high-momentum states beyond the momentum cutoff λ of the interaction but is not sufficiently extended in position space to accommodate a nucleus. For small values of $\hbar\omega$, the model space is sufficiently wide in position space for the extenson of the nucleus but does not contain sufficient high-momentum modes to resolve the cutoff λ of the interaction. Close to the minimum, in the largest model spaces considered, a good compromise is realized.

We also studied the energy levels using $V_{\text{low-}k}$ for various momentum cutoffs in the range $\lambda = 1.6$–2.2 fm^{-1}. The calculated ground-state energies for ^{16}O, ^{15}O, and ^{15}N are sensitive to the cutoff, implying that induced three-body forces and short-ranged forces of higher rank would contribute significantly to the calculated energies.

Let us turn to the spectroscopic factor for nucleon removal from ^{16}O. Figure 6 shows the spectroscopic factor, Eq. (25),

$$\text{SF}(1/2^-) \equiv S_{15}^{16}(l = 1, j = 1/2), \tag{30}$$

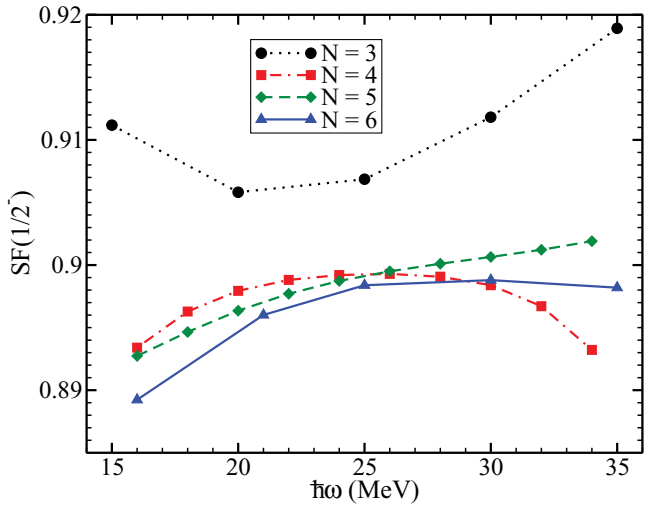

FIG. 6. (Color online) Spectroscopic factor SF($1/2^-$) for proton removal from ^{16}O as a function of the oscillator spacing $\hbar\omega$ for different model spaces consisting of $(N+1)$ oscillator shells and a low-momentum interaction with cutoff $\lambda = 2.0$ fm^{-1}.

for the removal of a proton with quantum numbers $J^\pi = 1/2^-$ from ^{16}O using a low-momentum interaction $V_{\text{low-}k}$ with a cutoff $\lambda = 2.0$ fm^{-1}. Evidently, the spectroscopic factor is well converged and depends very weakly on the size of the model space and the oscillator frequency $\hbar\omega$. It varies less than 1% over a wide range of oscillator frequencies. The spectroscopic factor SF($1/2^-$) for neutron removal from ^{16}O is almost identical to the SF($1/2^-$) for proton removal. Recall that isospin is approximately conserved in light nuclei.

The dependence on momentum cutoff λ is displayed in Fig. 7. Note that the spectroscopic factor increases with decreasing cutoff. This is expected, as upon lowering of the cutoff the system becomes less correlated, the product state $|\phi_0\rangle$ becomes an increasingly good approximation, and the

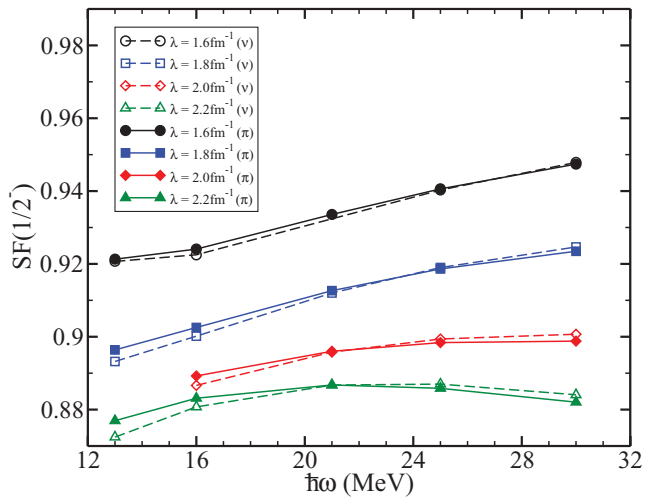

FIG. 7. (Color online) Spectroscopic factor SF($1/2^-$) for neutron and proton removal as a function of the oscillator spacing $\hbar\omega$ for nucleon-nucleon interactions with different cutoffs in a model space with $N = 6$.

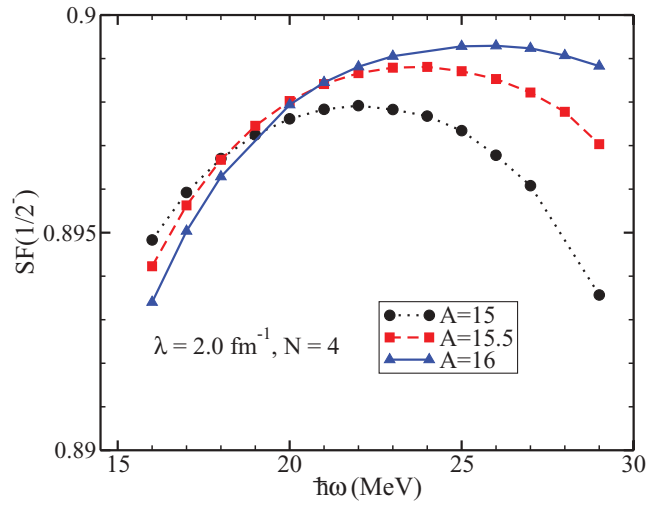

FIG. 8. (Color online) Spectroscopic factor SF($1/2^-$) for proton removal from ^{16}O as a function of the oscillator spacing $\hbar\omega$ computed for different values of the mass number A employed in the intrinsic Hamiltonian, Eq. (1). The model space consists of $N+1=5$ oscillator shells, and the momentum cutoff of the nucleon-nucleon interaction is $\lambda = 2.0$ fm^{-1}.

single-particle picture becomes more and more valid. Note also that isospin is approximately a good quantum number, as the spectroscopic factors for proton and neutron removal are almost identical.

Let us also study the center-of-mass problem. The intrinsic Hamiltonian, Eq. (1), depends on the mass number A of the nucleus, and the calculation of the spectroscopic factor requires us to employ identical Hamiltonians for nuclei with mass numbers A and $A-1$. This constitutes a dilemma, as no choice of actual value for the parameter A can satisfy the parent and daughter nuclei simultaneously. It is thus necessary to investigate how strongly the spectroscopic factor depends on this value. Figure 8 shows the spectroscopic factor (in a model space $N = 4$ for a momentum cutoff $\lambda = 2.0$ fm^{-1} for different values of the mass number A of the intrinsic Hamiltonian. The dependence on A is very weak, and it is similar in size to the dependence on the parameters of the model space.

For an *intrinsic* Hamiltonian, the coupled-cluster wave function of a closed-shell nucleus factorizes into an intrinsic part and a Gaussian for the center of mass coordinate [46]. Following the procedure in Ref. [46], we confirmed that this factorization is present for the ground states of ^{15}O and ^{15}N in the largest model space we considered. We found that this factorization even takes place if the value $A = 16$ for the mass number is employed in the intrinsic Hamiltonian, Eq. (1), for computation of the nuclei ^{15}O and ^{15}N. These results suggest that our approach to calculating spectroscopic factors within the coupled-cluster method is practically free of any center-of-mass contamination. In particular, it is not necessary to employ the corrections [28,47] that are caused by wave functions with spurious center-of-mass excitations.

So far, we have focused on the spectroscopic factors for removal of a $J^\pi = 1/2^-$ proton and neutron from ^{16}O. We finally also compute the spectroscopic factor for removal of a $J^\pi = 3/2^-$ proton and a (deeply bound) $J^\pi = 1/2^+$

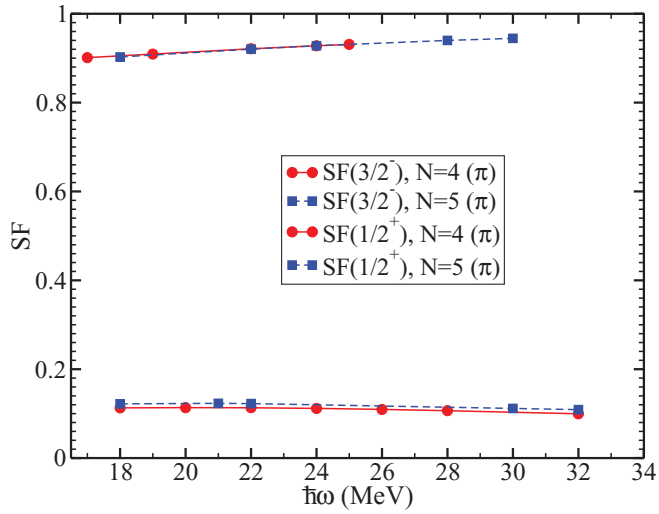

FIG. 9. (Color online) Spectroscopic factors SF($3/2^-$) and SF($1/2^+$) for proton removal from ^{16}O as a function of the oscillator spacing $\hbar\omega$. The employed model spaces have $N + 1$ oscillator shells, and the momentum cutoff of the nucleon-nucleon interaction is $\lambda = 2.0$ fm^{-1}.

proton from ^{16}O. The result is shown in Fig. 9 for different model spaces. As before, the results are well converged with respect to the size of the model space and display only a mild dependence on the oscillator frequency. We find that the spectroscopic factor SF($3/2^-$) is similar in size to SF($1/2^-$). This is an interesting result. Barbieri and Dickhoff [25] also found, in their computation of spectroscopic factors, that SF($1/2^-$) $\approx$ SF($3/2^-$) for nucleon removal from ^{16}O. As expected, the spectroscopic factor of the $J^\pi = 1/2^+$ state is very small. The removal of a deeply bound $J^\pi = 1/2^+$ proton from ^{16}O yields a highly excited state of ^{15}N that is a rather complex superposition of many n-particle–$(n + 1)$-hole states and thus has little overlap with a one-hole state.

V. CONCLUSION AND OUTLOOK

We have extended the coupled-cluster method for the computation of spectroscopic factors. To this purpose, we derived diagrammatic and algebraic expressions of the one-body overlap functions based on EOM methods for the ground and excited states of the closed-shell nucleus with mass number A and the neighboring nuclei with mass number $A - 1$. We implemented the equations in an uncoupled m scheme and presented proof-of-principle calculations of the spectroscopic factor for proton and neutron removal from ^{16}O. The calculated spectroscopic factors are well converged in model spaces consisting of six oscillator shells for low-momentum nucleon-nucleon interactions. Within the coupled-cluster approach, the same intrinsic Hamiltonian has to be employed in the nuclei with mass numbers A and $A - 1$. We found that the spectroscopic factor is insensitive to the actual value of the mass number that is employed in the intrinsic Hamiltonian.

We plan to implement the computation of the spectroscopic factor also in a spherical formulation of nuclear coupled-cluster theory. This will allow us to employ much larger model spaces, and we plan to apply the techniques to physically interesting nuclei, such as ^{22,24}O, ^{48,52}Ca, and ^{56,78}Ni.

ACKNOWLEDGMENTS

We acknowledge discussions with C. Barbieri, E. Bergli, R. J. Furnstahl, and M. Hjorth-Jensen. Ø.J. thanks the University of Oslo and Oak Ridge National Laboratory (ORNL) for hospitality. This research was partly funded by Norwegian Research Council Project NFR 171247/V30 and by the US Department of Energy under Grant Nos. DE-FG02-96ER40963 (University of Tennessee) and DE-FC02-07ER41457 (SciDAC UNEDF). This research used resources of the National Center for Computational Sciences at ORNL.

[1] P. Navrátil, J. P. Vary, and B. R. Barrett, Phys. Rev. C **62**, 054311 (2000).
[2] S. C. Pieper and R. B. Wiringa, Annu. Rev. Nucl. Part. Sci. **51**, 53 (2001).
[3] A. Nogga, A. Kievsky, H. Kamada, W. Glockle, L. E. Marcucci, S. Rosati, and M. Viviani, Phys. Rev. C **67**, 034004 (2003).
[4] C. Ordonez, L. Ray, and U. van Kolck, Phys. Rev. C **53**, 2086 (1996).
[5] P. Bedaque and U. van Kolck, Annu. Rev. Nucl. Part. Sci. **52**, 339 (2002).
[6] E. Epelbaum, H.-W. Hammer, and U.-G. Meißner, Rev. Mod. Phys. **81**, 1773 (2009).
[7] D. R. Entem and R. Machleidt, Phys. Rev. C **68**, 041001(R) (2003).
[8] S. K. Bogner, T. T. S. Kuo, and A. Schwenk, Phys. Rep. **386**, 1 (2003).
[9] S. K. Bogner, R. J. Furnstahl, and A. Schwenk, Prog. Part. Nucl. Phys. **65**, 94 (2010).
[10] P. Navrátil, V. G. Gueorguiev, J. P. Vary, W. E. Ormand, and A. Nogga, Phys. Rev. Lett. **99**, 042501 (2007).
[11] P. Navrátil, V. G. Gueorguiev, J. P. Vary, W. E. Ormand, A. Nogga, and S. Quaglioni, Few-Body Syst. **43**, 129 (2008).
[12] P. Navrátil, S. Quaglioni, I. Stetcu, and B. R. Barrett, J. Phys. G: Nucl. Part. Phys. **36**, 083101 (2009).
[13] E. Epelbaum, H. Krebs, D. Lee, and U.-G. Meißner, arXiv:1003.5697v1.
[14] G. Hagen, T. Papenbrock, D. J. Dean, and M. Hjorth-Jensen, Phys. Rev. Lett. **101**, 092502 (2008).
[15] C. Barbieri, Phys. Rev. Lett. **103**, 202502 (2009).
[16] S. Fujii, R. Okamoto, and K. Suzuki, Phys. Rev. Lett. **103**, 182501 (2009).
[17] G. Hagen, D. J. Dean, M. Hjorth-Jensen, and T. Papenbrock, Phys. Lett. B **656**, 169 (2007).
[18] K. M. Nollett, S. C. Pieper, R. B. Wiringa, J. Carlson, and G. M. Hale, Phys. Rev. Lett. **99**, 022502 (2007).
[19] S. Quaglioni and P. Navrátil, Phys. Rev. Lett. **101**, 092501 (2008).

[20] P. G. Hansen and J. A. Tostevin, Annu. Rev. Nucl. Part. Sci. **53**, 219 (2003).
[21] M. F. Macfarlane and J. B. French, Rev. Mod. Phys. **32**, 567 (1960).
[22] J. M. Bang, F. G. Gareev, W. T. Pinkston, and J. S. Vaagen, Phys. Rep. **125**, 253 (1985).
[23] R. J. Furnstahl and H. W. Hammer, Phys. Lett. B **531**, 203 (2002).
[24] R. J. Furnstahl and A. Schwenk, arXiv:1001.0328v1.
[25] C. Barbieri and W. H. Dickhoff, Int. J. Mod. Phys. A **24**, 2060 (2009).
[26] A. Polls, M. Radici, S. Boffi, W. H. Dickhoff, and H. Müther, Phys. Rev. C **55**, 810 (1997).
[27] W. J. W. Geurts, K. Allaart, W. H. Dickhoff, and H. Müther, Phys. Rev. C **53**, 2207 (1996).
[28] D. Van Neck, M. Waroquier, A. E. L. Dieperink, S. C. Pieper, and V. R. Pandharipande, Phys. Rev. C **57**, 2308 (1998).
[29] A. Fabrocini and G. Co', Phys. Rev. C **63**, 044319 (2001).
[30] F. Coester, Nucl. Phys. **7**, 421 (1958).
[31] F. Coester and H. Kümmel, Nucl. Phys. **17**, 477 (1960).
[32] J. Čížek, J. Chem. Phys. **45**, 4256 (1966).
[33] J. Čížek, Adv. Chem. Phys. **14**, 35 (1969).
[34] H. Kümmel, K. Lührmann, and J. Zabolitzky, Phys. Rep. **36**, 1 (1978).
[35] R. J. Bartlett and M. Musiał, Rev. Mod. Phys. **79**, 291 (2007).
[36] D. J. Dean and M. Hjorth-Jensen, Phys. Rev. C **69**, 054320 (2004).
[37] G. Hagen, D. J. Dean, M. Hjorth-Jensen, T. Papenbrock, and A. Schwenk, Phys. Rev. C **76**, 044305 (2007).
[38] G. Hagen, T. Papenbrock, D. J. Dean, M. Hjorth-Jensen, and B. Velamur Asokan, Phys. Rev. C **80**, 021306(R) (2009).
[39] S. K. Bogner, T. T. S. Kuo, and A. Schwenk, Phys. Rep. **386**, 1 (2003).
[40] K. Kowalski, D. J. Dean, M. Hjorth-Jensen, T. Papenbrock, and P. Piecuch, Phys. Rev. Lett. **92**, 132501 (2004).
[41] J. R. Gour, P. Piecuch, M. Hjorth-Jensen, M. Wloch, and D. J. Dean, Phys. Rev. C **74**, 024310 (2006).
[42] J. Geertsen, M. Rittby, and R. J. Bartlett, Chem. Phys. Lett. **164**, 57 (1989).
[43] D. J. Rowe, Rev. Mod. Phys. **40**, 153 (1968).
[44] R. F. Bishop, M. F. Flynn, M. C. Bosca, E. Buendia, and R. Guardiola, Phys. Rev. C **42**, 1341 (1990).
[45] B. Mihaila and J. H. Heisenberg, Phys. Rev. C **60**, 054303 (1999).
[46] G. Hagen, T. Papenbrock, and D. J. Dean, Phys. Rev. Lett. **103**, 062503 (2009).
[47] A. E. L. Dieperink and T. D. Forest, Phys. Rev. C **10**, 543 (1974).
[48] T. D. Crawford and H. F. Schaefer III, Rev. Comp. Chem. **14**, 33 (2000).
[49] E. Epelbaum, A. Nogga, W. Glöckle, H. Kamada, Ulf-G. Meißner, and H. Witała, Phys. Rev. C **66**, 064001 (2002).